Spatial Statistics 69 (2025) 100927

Contents lists available at ScienceDirect

Spatial Statistics

journal homepage: www.elsevier.com/locate/spasta

Regime changes and spatial dependence in the 2020 US presidential election polls

Giampiero M. Gallo [a,b], Demetrio Lacava [c,*], Edoardo Otranto [b,d]

[a] New York University in Florence, Via Bolognese, 120, Firenze, 50139, Italy
[b] CRENoS - Centro Ricerche Economiche Nord Sud, Via S. Giorgio, 12, Cagliari, 09124, Italy
[c] Department of Economics, University of Messina, via dei Verdi, 75, Messina, 98122, Italy
[d] Department of Social Sciences and Economics, Sapienza University of Rome, Viale dell'Università, 36, Rome, 00185, Italy

ARTICLE INFO

Keywords:
Electoral polls
Markov switching
Spatial dependence
Political spillover
Political contagion
Autoregressive model

ABSTRACT

This paper introduces a novel two-stage modeling framework that combines Markov Switching (MS) models with an autoregressive model augmented by spatial effects to analyze the dynamics and spatial interdependence of Biden's polling percentages during the 2020 electoral campaign. In the first stage, we employ MS models to segment each state's daily polling time series into distinct regimes — interpreted as phases of decline, stability, and growth. This segmentation captures abrupt changes and local trends in public opinion, enabling us to link regime shifts with key political events such as debates, party conventions, and milestone campaign achievements. The inherent nonlinearity of polling data would otherwise be lost by first differencing. By removing the regime-specific components, we generate stationary residuals modeled using an Autoregressive model with exogenous variables (ARX) that incorporates political spatial interactions through two complementary effects. The spillover effect captures lagged influences arising from politically influential states, while the contagion effect reflects the contemporaneous impact of neighboring states. A recursive algorithm based on partial correlations is implemented to select the most relevant spillover sources for each state. Empirical results, based on daily data from 13 swing states, reveal robust evidence of persistent regime structures and marked spatial dependencies. While contagion effects are uniformly significant across states, spillover dynamics exhibit considerable heterogeneity in both magnitude and direction. This integrated modeling approach enhances our understanding of the complex, nonlinear temporal evolution of polling trends and the spatial diffusion of political opinions that underpinned the 2020 electoral outcome.

1. Introduction

The analysis of successive outcomes in the US presidential election polls provides a valuable example of how political opinions may diffuse geographically. It reflects not only each candidate's popularity, but also the sociopolitical dynamics across neighboring states, supposedly sharing similar values. Thus, analyzing political contagion can offer key insights into the role of spatial interactions in shaping public opinions (see Berlemann and Enkelmann, 2014, for a survey on the economic determinants of the US presidential approval ratings).

The literature has long established that public opinions do not evolve in isolation, but are influenced by spatial interdependencies. Geographic, economic, and cultural connections between states (regions) are key factors in the diffusion of political opinions, as

* Corresponding author.
E-mail address: dlacava@unime.it (D. Lacava).

https://doi.org/10.1016/j.spasta.2025.100927
Received 17 April 2025; Received in revised form 18 June 2025; Accepted 6 August 2025
Available online 26 August 2025
2211-6753/

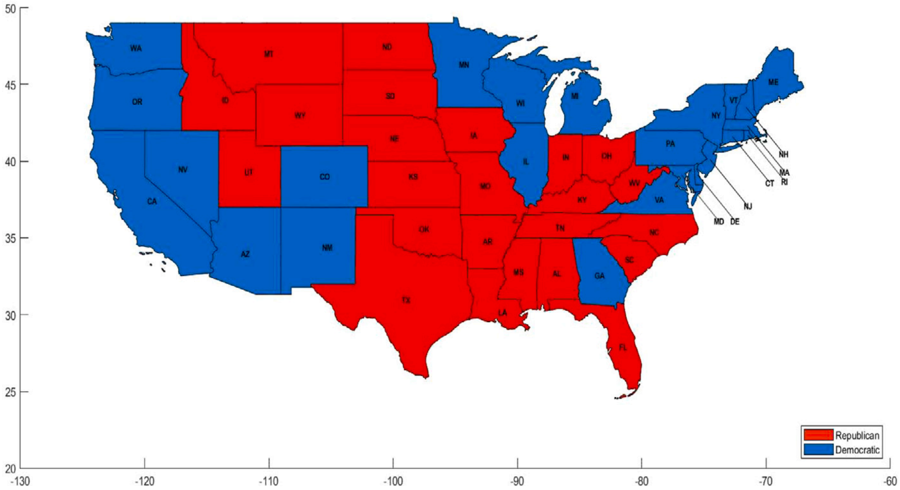

Fig. 1. 2020 U.S. Presidential Election State Results. The axes display geographical coordinates, with longitude on the x-axis and latitude on the y-axis.

highlighted by the theory of spatial diffusion. Previous research has shown that geographically adjacent states often exhibit similar political orientations, driven by structural factors such as demographic composition and regional economic conditions, as well as the effects of political contagion (Agnew, 1987; Pattie and Johnston, 2000). In such a context, Agnew (1987) emphasizes the importance of location in political behavior, suggesting that the geographic context plays a crucial role in shaping political interactions. Similarly, Pattie and Johnston (2000) explore how social interactions within local contexts can influence voting behavior, indicating that individuals who engage in political discussions within their communities are more likely to exhibit similar voting patterns. The current literature has explored the spatial dimensions of political behavior in the US, including voting patterns, presidential general election polling, and political attitudes. Wing and Walker (2010) show that presidential consensus ratings exhibit significant spatial dependencies, with neighboring states sharing similar approval levels due to factors such as media influence and regional contagion; Foley and Demšar (2013) provide a comprehensive review of spatial econometrics, highlighting how spatial analysis techniques could improve understanding of political behavior by accounting for spatial dependencies.

Let us examine the distribution of the US states assigned to Democrats and Republicans in the 2020 Presidential elections, reported in Fig. 1. The presence of spatial clustering is evident, since states with similar results are neighboring (with the notable exception of Georgia-GA, one of the key states for Biden's victory in 2020). We do not suggest a "structural" model that accounts for voter behavior and the possibility of voter change through interaction: the amount of information to consider for this purpose would be paramount and certainly hard to consider within a statistical model.

We favor a data-driven approach with relatively high frequency poll results by state in the months preceding the general elections in 2020. In our model, the dynamic spatial interdependence of the series of election polls across US states can be accommodated by a specification with spatial effects due to proximity (called contagion effects); by the same token, since media and information may produce relevant interaction effects on electoral choices even at a distance, we find it interesting to investigate whether changes in any US state can influence the behavior of other states. In principle, these effects could be more significant in the so-called swing states, defined as such due to a less stable allegiance to either party candidate in subsequent elections. A procedure identifies the most influential states via a selection algorithm: in this case the transmission occurs after the news has been spread and therefore we consider it in the form of spillover effects, i.e. with a lag.

Thus, the spatial interdependence of the US presidential election polls across US states is explored along two dimensions: (i) the political spillover — polls in a given state are influenced by lagged results in other prominent states selected regardless of geographic proximity; and (ii) the political contagion – a spatial component with a contemporaneous impact from neighboring states.

From a temporal point of view, the dynamics of the polls are modeled with regime changes capturing periods of decline, stability, and growth in preferences towards a candidate before the actual voting is expressed, in view of the abrupt changes one can observe after particular events occurring during the electoral campaign.

Using a data set of presidential general election polling series recorded in the so-called swing states in the 2020 presidential election campaign, we suggest a new procedure structured in two stages: the first employs Markov Switching models to identify distinct regimes (representing periods of decline, stability, and growth, respectively) in the time series of the polls, while the second adopts an autoregressive model with spatial effects that integrates political spillover and contagion. The former effect, in particular, requires identifying the states that may generate spillover effects for each state in our sample. To this end, we propose a novel recursive algorithm that uses significant partial correlations to determine the most relevant sources of spillover.

We manage to identify phases in which a candidate's support evolves in an increasing, decreasing, or stable manner; such dynamics appear to be closely linked to significant political events — such as reaching enough support for the nomination, the start of the Republican convention, and the presidential debates — and are further influenced by spatial dependence.

Table 1
Space–time correlations. Sample period May 20, 2020–November 3, 2020.

Space–time correlation												
Alabama	Arizona	California	Colorado	Connecticut	Delaware	Florida	Georgia	Indiana	Iowa	Kansas	Kentucky	Maine
0.455	0.035	0.664	0.324	0.794	0.869	0.231	0.329	0.491	0.482	0.534	0.098	0.239
Maryland	Massachusetts	Michigan	Minnesota	Mississippi	Missouri	Montana	Nebraska	Nevada	New Hampshire	New Jersey	New Mexico	New York
0.846	0.737	0.780	0.228	0.574	0.831	−0.027	0.551	0.808	0.458	0.553	0.148	0.858
North Carolina	North Dakota	Ohio	Oklahoma	Pennsylvania	South Carolina	Tennessee	Texas	Utah	Virginia	Washington	West Virginia	Wisconsin
0.832	0.101	−0.484	0.774	0.809	0.494	0.770	0.757	0.559	0.924	–	0.633	0.415

The remainder of the paper is structured as follows. Section 2 discusses the data set; Section 3 presents the main features of the proposed model; the empirical application is discussed in Section 4; finally, Section 5 provides some final remarks.

2. The 2020 US presidential election polls

US election results are generally characterized by a strong spatial clustering of states. As mentioned above, Fig. 1 shows the 2020 results in favor of the Democratic (blue) and Republican (red) candidate for each continental state.[1] Support by state is always clustered in contiguous areas; the only exception is Georgia, which was one of the key states in determining Biden's final victory: this swing state is surrounded by Republican states and in 2020 had a Republican Governor.

By the same token, the dynamics of the polls in the pre-election period show a non-linear behavior, as illustrated in Fig. 2.

To study the spatial–temporal characteristics of the polls, we used the daily survey data set provided by FiveThirtyEight.[2] Since the time series referring to the polls of different states have different lengths, we decided to collect only 39 states with a complete range of daily data available between May 20 and November 3 ($T = 168$ observations for each series — the 9 excluded states are represented in gray in Fig. 3 plus Alaska and Hawaii, not shown on the map).

The space–time relationships between each state j and its neighbors can be documented by the space–time correlations between the time series of that state and the time series obtained as a linear combination of its k_j neighbors with equal weights. Denoting with $\mathbf{y}_j$ the time series of percentage in favor of Biden in the state j, and with $\boldsymbol{Y}$ the corresponding matrix of time series for all 39 available states, the space–time correlation coefficient of state j is given by:

$$\rho_j^{ST} = Corr(\boldsymbol{y}_j, \boldsymbol{Y}\boldsymbol{w}_{c,j}) \tag{1}$$

where $\boldsymbol{w}_{c,j}$ is the weight vector referring to state j, with elements equal to $1/k_j$ if it refers to a neighbor, and 0 otherwise. Table 1 shows the space–time correlations for each state, which are very high for Virginia (0.924), New York (0.858) and North Carolina (0.832), and suggest that nearby regions significantly influence polling trends in these states. However, Ohio (−0.484) is notable for a negative correlation, suggesting an inverse relationship between its polling trends and those of its neighboring states. This could reflect different political or demographic factors influencing Ohio, compared to its surrounding states. Taking a look at other key states in the 2020 presidential election, it emerges that Arizona (0.035), Florida (0.231), and Georgia (0.329) show weaker correlations with neighboring states.

Overall, the diverse range of space–time correlations for these states provides valuable insights into the spatial–temporal evolution of US electoral preferences, reflecting how different regions may share or diverge in the dynamics of their political opinions.

In the empirical analysis, we focus on the 13 swing states identified by *Ballotpedia*.[3] These are the states where no candidate had overwhelming support in 2020 and whose final vote decided Biden's overall victory: Arizona-AZ, Florida-FL, Georgia-GA, Iowa-IA, Michigan-MI, Minnesota-MN, Nevada-NV, New Hampshire-NH, North Carolina-NC, Ohio-OH, Pennsylvania-PA, Texas-TX, and Wisconsin-WI. In Fig. 3 they are identified by faded red tones if the final vote favored Trump (FL, IA, NC, OH, TX), faded blue tones if the final vote favored Biden (AZ, GA, MI, MN, NH, NV, PA, WI). All swing states border both red and blue states, except for NH, which is surrounded only by blue states, and GA, which is surrounded only by red states; this seems to be another sign of the spatial characterization of the vote distribution. In this regards, Fig. 2 shows the dynamics of the 13 time series of support for Biden in swing states, clearly characterized by non-linear trends, with phases of increase, decrease, and stability. However, it should be noted that the prevailing behavior seems idiosyncratic, although some turning points correspond to certain dates. All series show an increase after the end of May and a collapse in July, often in the middle of the month. In the last part of the period considered, with the effort of the electoral campaign at its peak, the series show very different behaviors: there are states with a final decreasing trend (IA, OH, PA), stability (AZ, FL, NH, NC, NV), and states that have a sharp final increase after a decreasing trend (GA, MI, MN, TX, WI). Overall, these dynamics seem consistent with the presence of regimes that drive changes in the level and slope of the series.

[1] Alaska (Republican) and Hawaii (Democratic) are not present on the map.

[2] Now available at https://github.com/fivethirtyeight/data/tree/master/polls/2024-averages.

[3] Quoting Wikipedia, "Ballotpedia is a nonprofit and nonpartisan online political encyclopedia that covers federal, state, and local politics, elections, and public policy in the United States".

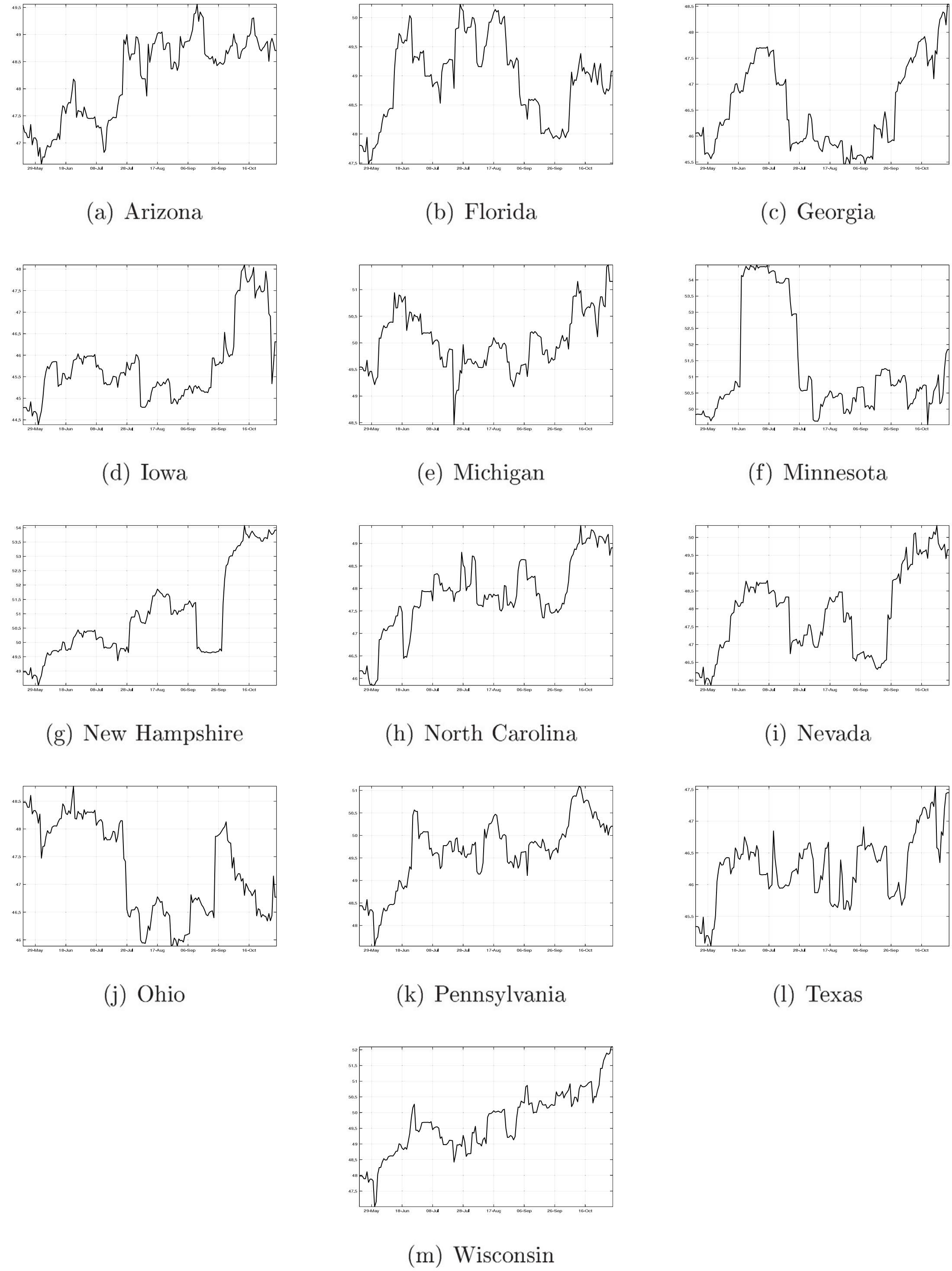

Fig. 2. Percentage support for Biden in various states (2020 polls). Sample period May 20, 2020–November 3, 2020.

3. The methodological approach: a 2-stage model

The empirical evidence provided points to a clear spatial effect, the presence of regimes, with some common dynamics but a prevailing idiosyncratic behavior. This can be accommodated with a novel 2-stage univariate time series model with regime shifts

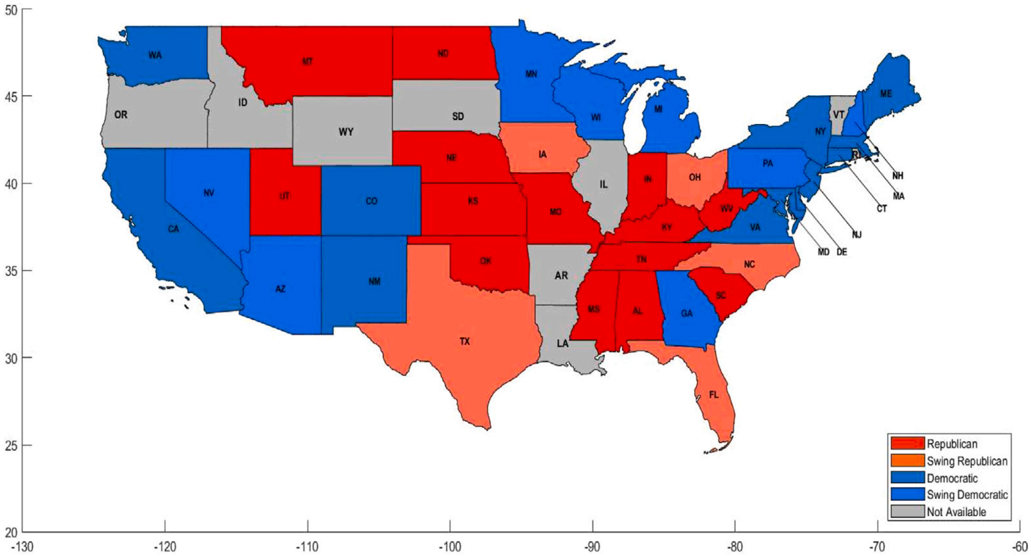

Fig. 3. 2020 U.S. Presidential Election State Results; colored (blue and red) states are considered for the analysis, gray states are excluded. Swing states in faded blue and red tones. The axes display geographical coordinates, with longitude on the x-axis and latitude on the y-axis.

and spatial effects. The 13 series shown in Fig. 2 are nonstationary, as detected by the Augmented Dickey–Fuller (ADF) test. The usual operations to make the series stationary, such as first differences, would create a series of daily variations of the polls, losing the pattern of apparent local trends characterizing these series as subject to regimes. Our idea is to use a first stage to capture the local trends of the series with a Markov Switching (MS) model (Hamilton, 1994, Ch. 22), inferring the turning points via the so-called smoothed probabilities. This has the double advantage of distinguishing the different regimes for each series and of obtaining stationary series by subtracting the local trends from the original series. In the second stage, the transformed series are modeled using autoregressive dynamics (AR) with spatial effects that capture the transmission of variations in the polls from other states. As already mentioned, we are defining political spillover and contagion effects: the first captures the influence in the polls in a given state from lagged results in other prominent states selected, regardless of geographic proximity; the second represents a spatial component with a contemporaneous impact from neighboring states.

The proposed model can help answer two questions of interest to political analysts:

1. Are regimes consistent with events that might have affected the electorate?
2. Does the outcome of swing states depend on spatial effects?

3.1. First stage: The detection of regimes

Let $y_{j,t}$ be the logarithm of the poll result in favor of Biden in the swing state j recorded on day t. We fit a different linear trend corresponding to each unobservable regime, represented by a discrete random variable $s_{j,t} \in \{1,\dots,s\}$; for example, in the case $s=3$, label 1 represents the declining regime, 2 stable, and 3 increasing, respectively. To this end, we adopt an s-state MS model:

$$y_{j,t} = \alpha_{j,s_{j,t}} + \beta_{j,s_{j,t}} t + \varepsilon_{j,t}, \quad \varepsilon_{j,t} \sim \text{i.i.d. } \mathcal{N}(0, \sigma^2_{j,s_{j,t}}) \qquad t = 1,\dots,T \tag{2}$$

where $\alpha_{j,s_{j,t}}$ and $\beta_{j,s_{j,t}}$ represent the regime-specific intercept and time slope, respectively. The variance of the disturbance $\varepsilon_{j,t}$ is also assumed to change with $s_{j,t}$ to capture the possible heteroskedasticity related to the regime shift.

As said, $s_{j,t}$ is not observable, but it is supposed to evolve as a first-order Markov chain with transition probabilities:

$$p^{(j)}_{ih} = \Pr\left[s_{j,t} = h \mid s_{j,t-1} = i\right], \quad \sum_{h=1}^{s} p^{(j)}_{ih} = 1 \quad \forall i. \tag{3}$$

Let $\mathcal{I}_r$ be the set of information available at time r. Maximum likelihood estimation can be performed by applying the Hamilton filter (Hamilton, 1990), a recursive procedure, similar to a Kalman filter with discrete state variable, which provides, at each step, the conditional density of $y_{j,t}$ as a mixture of s Normal pdf's with weights given by the predicted probabilities $\Pr(s_{j,t} = h \mid \mathcal{I}_{t-1})$ $(h = 1,\dots,s)$.

Regime inference can be provided via Kim smoother (Kim, 1994), a recursive estimate of the state probability, obtained by moving backward through the data. The Kim smoother provides, for each t, the smoothed probability $\Pr(s_{j,t} = h \mid \mathcal{I}_T)$, that is, the probability of each regime h conditional on the full information available. This tool can be used to assign each observation $y_{j,t}$ to the regime identified by the mode of the smoothed probability distribution of $s_{j,t}$.[4] The classification of observations into regimes helps to interpret the different phases of the electoral trend in each state, and in particular whether regime changes are consistent with particular events relevant to the electoral campaign.

3.2. Second stage: The detection of spatial effects

The stationary series we work with in the second stage are obtained by standardizing the original series by the MS local trend and regime-specific heteroskedastic effects:

$$\hat{\varepsilon}_{j,t} = \frac{y_{j,t} - \sum_{h=1}^{s}\left(\hat{\alpha}_{j,h} + \hat{\beta}_{j,h} t\right)}{\hat{\sigma}_{j,h}} Pr(s_{j,t} = h|\mathcal{I}_T) \tag{4}$$

where a hat indicates the estimated value. We model these series considering both spatial and temporal effects. As mentioned in Section 1, the choice of spatial weights is strictly connected to the spatial pattern illustrated in Fig. 1 and to the transmission mechanisms that regulate the dynamics of electoral preferences. In practice, the choice of weight matrices derives from the type of mechanisms we want to investigate. The weights related to the most influential states can be obtained through a data-driven algorithm, illustrated at the end of this section. On the other hand, to capture spatial clustering effects, we resort to the typical consideration of equal weights in correspondence with neighbors (cf. the seminal works of Moran, 1948; Geary, 1954, who proposed the notion of binary contiguity between spatial units).[5] The use of two different spatial matrices to capture separate effects in the same model provides a useful framework to the empirical analysis (see, e.g., Elhorst et al., 2012).

These weight structures are included in an autoregressive model enriched by the spatial effects of spillover and contagion:

$$\hat{\varepsilon}_{j,t} = \omega_j + \varphi_j \hat{\varepsilon}_{j,t-1} + \theta_{s,j} \Delta \mathbf{y}_{t-1} \mathbf{w}_{s,j} + \theta_{c,j} \Delta \mathbf{y}_t \mathbf{w}_{c,j} + u_{j,t}, \qquad u_{j,t} \sim iiN(0, \sigma^2) \tag{5}$$

where $\{\omega_j, \varphi_j, \theta_{s,j}, \theta_{c,j}\}$ is the set of coefficients of the equation of state j; $\mathbf{y}_t$ is the t–th row of the presidential poll data matrix for all states $\mathbf{Y}$; Δ denotes the difference operator; $\mathbf{w}_{s,j}$ is the spatial weight vector to select and weigh the most influential states of j; $\mathbf{w}_{c,j}$ is the weight vector as defined in Section 2 after Eq. (1). Finally, $u_{j,t}$ is the error term which is assumed to be white noise and normally distributed.

It is important to underline that on the right-hand side of Eq. (5) we consider the first differences of the variables representing the polls of neighbors and influential states and not the residuals obtained by detrending these series with MS models, as for the dependent variable. The main issue is that swing states follow different changepoints.[6] Therefore, eliminating in the first step the influence of regimes from the dependent variable aims at isolating a more interesting variable (the residual) to study its evolution. In its dynamic model what we put on the right-hand side should contain — apart from the own past — changes in the original poll outcomes in other states (neighbors and influential states). By maintaining such original variables ($\mathbf{y}$), we leave to the empirical investigation the possibility to capture the full evolution of the other states' polls including the effects of changes in their own regimes as an element that could spur imitation in the state under exam.[7]

The model (5) is thus an ARX model with exogenous variables represented by the lagged variations in the polls in favor of Biden in the other states (spillover) and by the spatial contemporaneous impact coming from neighboring states (contagion) that captures the pattern illustrated in Figs. 1 and 3.

We propose a recursive algorithm based on forward selection in a stepwise regression to select the states most influential to j and construct the vector $\mathbf{w}_{s,j}$. The idea of the algorithm is to select, at each step, the variable in the matrix $\Delta \mathbf{Y}_t$ that has a significant partial correlation (that is, netting out the effect of other variables already considered) with $\hat{\varepsilon}_{j,t}$. Let $\mathbf{X}_t$ be the matrix that contains all the series in $\Delta \mathbf{Y}_t$ excluding the jth. In detail, the algorithm consists of the following steps:

1. Compute $Corr(\hat{\varepsilon}_{j,t}, \mathbf{X}_{t-1})$; let x^*_{t-1} be the variable that provides the highest correlation.
2. Regress $\hat{\varepsilon}_{j,t}$ on x^*_{t-1}, calculate the p-value on its t-stat and the adjusted determination coefficient $\bar{R}^2$:
   (a) If the p-value $\geq \alpha$ (the significance level chosen), **Stop** – No spillover effect is detected and the weights $\mathbf{w}_{s,j}$ are set to zero.
   (b) If the p-value $< \alpha$, **Start the procedure** – Insert x^*_t into the matrix $\mathbf{Z}_{t-1}$ and all the remaining variables from $\mathbf{X}_{t-1}$ into the matrix $\mathbf{V}_{t-1}$.
3. Regress $\hat{\varepsilon}_{j,t}$ on $\mathbf{Z}_{t-1}$, save the residuals ξ_t and compute $\bar{R}^2$.
   If $\bar{R}^2$ does not improve, **go to 7**.
4. Regress each variable in $\mathbf{V}_{t-1}$ on $\mathbf{Z}_{t-1}$ and save the residuals in the matrix $\mathbf{E}_{t-1}$.

[4] For details on MS model estimation and filtering and smoothing procedures, we refer to Hamilton (1994), Ch. 22.

[5] Given the clear effects of immediate neighbors illustrated in Fig. 1, we prefer to adopt this type of weights. Other typical alternatives, such as contiguity-based, distance-based, or k–nearest neighbors weight matrices, could be also adopted (Anselin, 2013).

[6] As we will show in the empirical results of Section 4, the comparison for the classification of regimes for each pair of states points out that detected regimes are generally out of sync.

[7] Further empirical evidence on the advantages of using first differences (and the disadvantages of using residuals) is not included in this paper, but is available upon request.

5. Compute $Corr(\xi_t, \boldsymbol{E}_{t-1})$ and insert e^*_{t-1} with the highest correlation in $\boldsymbol{Z}_{t-1}$ and eliminate the corresponding x^*_{t-1} from $\boldsymbol{V}_{t-1}$. If $\boldsymbol{V}_{t-1}$ is empty, **go to 7**.
6. **Go to 3**.
7. Compute the first principal component of the matrix $\boldsymbol{X}_{t-1}$ excluding the corresponding variables in $\boldsymbol{V}_{t-1}$, and the weights $\boldsymbol{w}_{s,j}$ as its squared loadings (which sum to 1).

In step 2, the selection of the first influential state is provided, which depends on the choice of the significance level α. Higher values of α will favor the identification of the first influential state, while lower values may end up not determining any influential state: we suggest as a good compromise $\alpha = 0.10$.

4. Empirical analysis

The empirical analysis is based on daily presidential polls in favor of Biden in the 13 swing states during the 2020 US presidential election, covering the period from May 20, 2020 to November 3, 2020. We carry out some preliminary analyses to statistically verify whether the characteristics of the series are consistent with our hypotheses of non-stationarity and the presence of regimes.

Considering the logarithms of the series to reduce their variability, the hypothesis of nonstationarity (unit root) is verified by the augmented Dickey–Fuller (ADF) test (Dickey and Fuller, 1979). The presence of a unit root is evident since the null hypothesis of a unit root is never rejected at any usual level of significance (first column of Table 2).

Identification of the number of regimes in a time series is subject to the problem of nuisance parameters present only under the alternative hypothesis (see, e.g., Hansen, 1992). The use of AIC and/or BIC might suggest the most suitable model, but should be used with caution, because they perform well only when the length of the series is large and the differences in the switching parameters are large (Psadarakis and Spagnolo, 2003, 2006; Otranto and Scaffidi Domianello, 2025). A simple method has recently been proposed by Otranto and Scaffidi Domianello (2025) investigating the similarity between smoothed probability in MS models and the membership grade in fuzzy clustering (see, e.g., D'Urso, 2015). They propose identifying the number of regimes using typical cluster validation indices applied to alternative fuzzy clusters with a different number of groups. The validation indices considered are the Partition Coefficient (PC), the Partition Entropy (PE), the Modified Partition Coefficient (MPC), the Average Silhouette Width (ASW), the Average Silhouette Width Fuzzy (ASWF), and the Xie-Beni (XB) (for details on these indices, see Otranto and Scaffidi Domianello, 2025). The indices can provide different results; as shown by Otranto and Scaffidi Domianello (2025), PC and PE favor a lower number of regimes, while ASW and ASWF seem more robust in the presence of autocorrelated patterns. In general, a suitable approach is based on choosing the number of regimes identified by most validation indices, reminiscent of the *ensemble learning* developed in the machine learning framework (see, e.g., Dong et al., 2020).

We perform this procedure by pitting 2 against 3 regimes (considering a larger number of regimes would be unfeasible due to the small number of observations in the time series). Table 3 shows that for 10 of 13 series, all indices identify 3 regimes; for New Hampshire and North Carolina, 4 indices favor 3 regimes, while PC and PE 2. As mentioned above, these two indices tend to select a parsimonious number of states. Ohio is the only state subject to only two regimes. Consequently, following the ensemble learning criterion, we consider 3 regimes, interpretable as periods of decline, stability, growth for the polls in favor of Biden, for all the swing states, excluding Ohio, for which we estimate a MS model with 2 regimes (interpretable as periods of decline and stability, respectively).

4.1. First stage estimation

As described in Section 3, the first stage of our approach uses MS models to capture local trends in each series. Table 4 shows the estimation of the 13 MS models; regime labels are assigned a posteriori, after evaluating the intercept and slope in each regime to obtain a suitable interpretation of decline (regime 1), stability (regime 2), and growth (regime 3).

As shown in Table 4, the intercept and slope coefficients are significant at the 5% level, with a few sporadic exceptions: $\hat{\beta}_1$ is not significant for Florida and Iowa; $\hat{\beta}_2$ is not significant for Nevada, while it is significant at the 10% level for North Carolina. This implies an approximately flat behavior of the trend during the phases of that regime. For this reason, we constrained the non-significant slopes of Florida, Iowa, and Nevada to zero, resulting in regimes that can be interpreted as level shifts rather than trends.

The transition probabilities entering the estimation process are p_{11}, p_{12}, p_{21}, p_{22}, p_{32}, p_{33}; the remaining probabilities (p_{13}, p_{21}, p_{31}) are obtained from the unit add-up constraint illustrated in Eq. (3). Some estimates of the transition probabilities are equal to 0, which violates the regularity conditions we need for MS models, causing a singular Hessian of the log-likelihood; to compute the standard errors, we impose these probabilities to be equal to zero (see Hamilton and Susmel, 1994).

Generally, the probability of remaining in the same regime is very high: in particular, regime 1 is the most persistent (with $\hat{p}_{11}$ ranging from 0.89 for North Carolina to 0.99 for Michigan) in 4 out of 13 cases. Regime 3 is the most persistent in 6 of 13 cases, with $\hat{p}_{33}$ ranging from 0.78 to 0.98. Finally, regime 2 has the highest transition probability only in Arizona (0.95), Florida (0.96), and Georgia (0.98). Focusing on the cases where none of the transition probabilities are set to zero, when the process is in the declining regime, it is more likely to transition into the growing regime rather than into stability, with $p_{13} > p_{12}$ in Georgia and Minnesota. Furthermore, Georgia and Texas appear to be the states where Biden's consensus is more sensitive when the process is in the growing regime, with $p_{31} > p_{32}$. During stability periods, it is most likely to move into the growing regime in Florida, Michigan, Minnesota, and Nevada where $p_{23} > p_{21}$. Finally, Minnesota is the state where Biden's consensus remains the most stable over the

Table 2
Augmented Dickey–Fuller test p-value for the log of the original series, $y_{j,t}$, and the 1-Stage standardized residuals $\hat{\epsilon}_{j,t}$. Sample period May 20, 2020–November 3, 2020.

State	$y_{j,t}$	$\hat{\epsilon}_{j,t}$
Arizona	0.3564	0.0000
Florida	0.3639	0.0000
Georgia	0.9679	0.0000
Iowa	0.5510	0.0002
Michigan	0.5980	0.0000
Minnesota	0.5852	0.0000
Nevada	0.6579	0.0000
New Hampshire	0.3955	0.0000
North Carolina	0.2809	0.0000
Ohio	0.5226	0.0000
Pennsylvania	0.3460	0.0000
Texas	0.1990	0.0000
Wisconsin	0.2749	0.0000

Table 3
Detecting the number of regimes using partition indices. Sample period May 20, 2020–November 3, 2020.

State	PC	PE	MPC	ASW	ASWF	XB
Arizona	3	3	3	3	3	3
Florida	3	3	3	3	3	3
Georgia	3	3	3	3	3	3
Iowa	3	3	3	3	3	3
Michigan	3	3	3	3	3	3
Minnesota	3	3	3	3	3	3
Nevada	3	3	3	3	3	3
New Hampshire	2	2	3	3	3	3
North Carolina	2	2	3	3	3	3
Ohio	2	2	2	2	2	2
Pennsylvania	3	3	3	3	3	3
Texas	3	3	3	3	3	3
Wisconsin	3	3	3	3	3	3

Table 4
First stage: MS estimated coefficients with robust standard error (White, 1980) in parentheses. Sample period: 20 May, 2020–November 3, 2020.

(a)	Arizona	Florida	Georgia	Iowa	Michigan	Minnesota	Nevada	New Hampshire	North Carolina	Ohio	Pennsylvania	Texas	Wisconsin
α_1	−0.7503	−0.7287	−0.7742	−0.7925	−0.7218	−0.573	−0.6965	−0.5398	−0.7764	−0.7235	−0.7277	−0.7917	−0.7403
	(0.0026)	(0.0010)	(0.0013)	(0.0013)	(0.0026)	(0.0029)	(0.0014)	(0.0067)	(0.0012)	(0.0001)	(0.0011)	(0.0011)	(0.0019)
α_2	−0.7596	−0.6963	−0.7543	−0.7700	−0.7052	−0.5998	−0.7464	−0.7203	−0.7562	−0.8038	−0.7153	−0.7935	−0.7269
	(0.0016)	(0.0017)	(0.0017)	(0.0009)	(0.0018)	(0.0031)	(0.0018)	(0.0022)	(0.0015)	(0.0063)	(0.0017)	(0.0007)	(0.0008)
α_3	−0.7140	−0.7428	−0.7863	−0.9335	−0.7057	−0.6902	−0.7769	−0.7125	−0.7467		−0.7210	−0.7700	−0.7159
	(0.0116)	(0.0014)	(0.0005)	(0.0245)	(0.0023)	(0.0015)	(0.0016)	(0.0013)	(0.0014)		(0.0092)	(0.0009)	(0.0019)
β_1	0.0368	0.0000	−0.0057	0.0000	0.0258	−0.0784	−0.0582	−0.1262	0.0273	−0.0234	0.0243	0.0266	0.0388
	(0.0023)		(0.0017)		(0.0023)	(0.0035)	(0.0016)	(0.0068)	(0.0012)	(0.0011)	(0.0010)	(0.0009)	(0.0022)
β_2	0.0286	−0.0107	0.0105	−0.0209	0.0387	−0.0376	0.0000	0.0462	0.0181	0.0395	0.0263	0.0102	0.0350
	(0.0011)	(0.0012)	(0.0017)	(0.0009)	(0.0070)	(0.0025)		(0.0070)	(0.0018)	(0.0063)	(0.0020)	(0.0007)	(0.0007)
β_3	−0.0717	0.0549	0.0235	0.1236	0.1016	0.0042	0.0503	0.0581	0.0219		0.0416	0.0031	0.0354
	(0.0260)	(0.0021)	(0.0007)	(0.0173)	(0.0101)	(0.0016)	(0.0013)	(0.0009)	(0.0011)		(0.0206)	(0.0012)	(0.0017)
p_{11}	0.9307	0.9461	0.9578	0.9502	0.9947	0.9388	0.9554	0.9643	0.8901	0.9841	0.9442	0.8943	0.9177
	(0.0361)	(0.0263)	(0.0189)	(0.0154)	(0.0036)	(0.0341)	(0.0243)	(0.0377)	(0.0454)	(0.0099)	(0.0220)	(0.0453)	(0.0244)
p_{12}	0.0561	0.0539	0.0090	0.0498	0.0044	0.0288	0.0446	0.0357	0.1099	0.0159	0.0000	0.0000	0.0723
	(0.0329)	(0.0012)	(0.0077)	(0.0154)	(0.3095)	(0.0188)	(0.0041)	(0.0333)	(0.0454)	(0.0099)		(0.0000)	(0.0222)
p_{13}	0.0132	0.0000	0.0332	0.0000	0.0009	0.0325	0.0000	0.0000	0.0000		0.0558	0.1057	0.0100
p_{21}	0.0518	0.0112	0.0000	0.0628	0.0122	0.0493	0.0360	0.0000	0.0000	0.0199	0.0559	0.0000	0.1083
p_{22}	0.9482	0.9552	0.9783	0.9194	0.9556	0.8907	0.9113	0.9067	0.8969	0.9801	0.9441	0.8906	0.8580
	(0.0210)	(0.0170)	(0.0136)	(0.0338)	(0.0418)	(0.0608)	(0.0313)	(0.0508)	(0.0371)	(0.0130)	(0.0248)	(0.0476)	(0.0431)
p_{23}	0.0000	0.0336	0.0217	0.0178	0.0322	0.0599	0.0526	0.0933	0.1031		0.0000	0.1094	0.0337
	(0.0187)	(0.0002)	(0.0353)	(0.0001)	(0.0336)	(0.0513)	(0.0196)	(0.0962)	(0.0371)		(0.0482)	(0.1268)	(0.0252)
p_{31}	0.0000	0.0225	0.1795	0.0305	0.0000	0.0080	0.0000	0.0192	0.0411		0.0817	0.0542	0.0000
p_{32}	0.0561	0.0508	0.0426	0.0000	0.0715	0.0163	0.0387	0.0225	0.0000		0.1043	0.0439	0.0739
	(0.0446)	(0.0009)	(0.0373)	(0.0180)	(0.3139)	(0.0109)	(0.0028)	(0.0207)			(0.0606)	(0.0421)	(0.0527)
p_{33}	0.9439	0.9267	0.7778	0.9695	0.9285	0.9757	0.9613	0.9583	0.9589		0.8140	0.9019	0.9261
	(0.0446)	(0.0291)	(0.0889)	(0.0241)	(0.0562)	(0.0132)	(0.0124)	(0.0154)	(0.0182)		(0.0708)	(0.0273)	(0.0352)
σ_1^2	0.0054	0.0053	0.0049	0.0100	0.0071	0.0029	0.0034	0.0106	0.0047	0.0056	0.0035	0.0022	0.0069
	(0.0011)	(0.0005)	(0.0005)	(0.0007)	(0.0004)	(0.0009)	(0.0003)	(0.0006)	(0.0005)	(0.0005)	(0.0003)	(0.0003)	(0.0005)
σ_2^2	0.0039	0.0063	0.0071	0.0021	0.0058	0.0068	0.0108	0.0064	0.0032	0.0106	0.0039	0.0023	0.0021
	(0.0004)	(0.0005)	(0.0004)	(0.0003)	(0.0008)	(0.0008)	(0.0009)	(0.0019)	(0.0004)	(0.0006)	(0.0003)	(0.0003)	(0.0002)
σ_3^2	0.0025	0.0034	0.0016	0.0114	0.0022	0.0081	0.0053	0.0036	0.0061		0.0171	0.0052	0.0050
	(0.0006)	(0.0005)	(0.0003)	(0.0011)	(0.0006)	(0.0005)	(0.0006)	(0.0005)	(0.0004)		(0.0015)	(0.0004)	(0.0009)

Table 5
Adjusted Rand Index for the classification of regimes between pair of states.

	AZ	FL	GA	IA	MI	MN	NV	NH	NC	OH	PA	TX
Florida	0.336											
Georgia	0.406	0.406										
Iowa	0.441	0.328	0.356									
Michigan	0.485	0.403	0.431	0.359								
Minnesota	0.475	0.399	0.419	0.371	0.475							
Nevada	0.385	0.352	0.342	0.447	0.377	0.429						
New Hampshire	0.322	0.442	0.445	0.331	0.359	0.385	0.356					
North Carolina	0.316	0.403	0.473	0.324	0.417	0.375	0.333	0.365				
Ohio	0.449	0.424	0.611	0.359	0.521	0.435	0.344	0.489	0.440			
Pennsylvania	0.409	0.395	0.377	0.330	0.479	0.422	0.309	0.357	0.379	0.383		
Texas	0.325	0.369	0.388	0.317	0.354	0.361	0.360	0.371	0.445	0.387	0.326	
Wisconsin	0.405	0.327	0.401	0.346	0.450	0.429	0.332	0.404	0.326	0.378	0.350	0.299

sample period, with a higher probability of transitioning into the growing regime from both the declining and stability regimes, i.e. $p_{13} > p_{12}$ and $p_{23} > p_{21}$. Similarly, when in the growing regime, it is more likely to transition to stability than to the declining regime ($p_{32} > p_{31}$, in Minnesota, New Hampshire, and Pennsylvania).

Ohio is a special case, since MS(2) is preferred over MS(3) (see Table 3): in line with the subsequent election outcome, the declining regime is the most persistent, with a longer average duration[8] (62 days) compared to the stability regime (50 days). Regime 1 also exhibits a lower variance, indicating less variability during the declining period.

The primary purpose of this stage is to identify the regimes that characterize the dynamics of the 13 series. Based on the smoothed probabilities $Pr(s_{j,t} = h|\mathcal{I}_T)$, obtained by the filtering and smoothing procedure (see Hamilton, 1994), we can perform inference on the regimes.

Fig. 4 shows the evolution of the original series (on the left axis) together with the estimated regimes (right axis) and some exogenous events related to the electoral campaign (red vertical dashed-lines).

The heterogeneity in regimes is evident at first glance, highlighting that preferences for either candidate primarily depend on the socio-cultural factors of each state. This is further confirmed by the adjusted Rand Index (Rand, 1971; Hubert and Arabie, 1985), which is calculated based on the classification of regimes between pairs of states. The maximum value of the index is 1, which corresponds to a perfect match between two classifications. It is 0 when the units (the 13 states in our case) are randomly assigned to the groups; it may take negative values when the two classifications have less in common than when the units are randomly assigned (a very rare case). As shown in Table 5, the adjusted Rand Index is generally between 0.3 and 0.5, with a maximum of 0.611 between Georgia-GA and Ohio-OH, indicating a moderate level of similarity in the classification of the regimes between the states considered.

The most evident changes in regime can be related to some electoral-exogenous events. We identify four events that seem associated with regime changes (at least within a 10-day window): (1) Biden reaches the delegate threshold (May 26, 2020); (2) the beginning of the Republican convention (August 24); (3) the presidential debate (September 29); (4) the vice-presidential debate (October 7). For instance, the presidential debate corresponds to a switch towards regime 1 only in Ohio, while it had the opposite effect (regime 3) in Florida, Georgia, Iowa, New Hampshire, North Carolina, Pennsylvania, and Texas. Additionally, the start of the Republican National Convention led to a growth in Biden's support in Texas, while causing a decline in Florida, Iowa, Nevada, New Hampshire, Pennsylvania, and Wisconsin. Despite some differences in the classification and the reaction to exogenous events, the similar trajectories observed in different (both neighboring and non-neighboring) states support the idea that presidential polling data are sensitive to both spillover and contagion effects.

4.2. Second-stage estimation results

The first-stage filtering of the original log-series, taking into account the regime dependence (Eq. (4)) is effective in obtaining stationarity. The rejection of the unit root hypothesis, based on the ADF test (second column of Table 2), is widespread: the p-values are well below the 5% threshold for all series.

The second stage of the estimation process involves identifying the vectors of spatial weights $\boldsymbol{w}_c$ and $\boldsymbol{w}_s$ in Eq. (5). The latter refers to the spillover effect and requires identifying the set of the most influential states, which is obtained by applying the proposed recursive algorithm illustrated at the end of Section 3.2, at a significance level $\alpha = 0.10$.[9]

For each swing state, Table 6 displays the list of influential states, i.e., the sources of spillover effects, together with their weights (in parentheses). Florida appears to be influenced by Arizona, Missouri, and Pennsylvania — an alignment that may stem from common socio-demographic characteristics, such as a high share of older residents, the presence of politically volatile suburban

[8] The average duration in a regime h is estimated as $(1 - \hat{p}_{hh})^{-1}$.

[9] To further support the choice of the significance level, we conducted some evaluation of the sensitivity of the results to different choices of α. We estimated model (5) by identifying different influential states at different values of α, obtaining that the estimates of other coefficients (ω, φ, θ_c) are quite robust to the choice of α. The results of these experiments are available upon request.

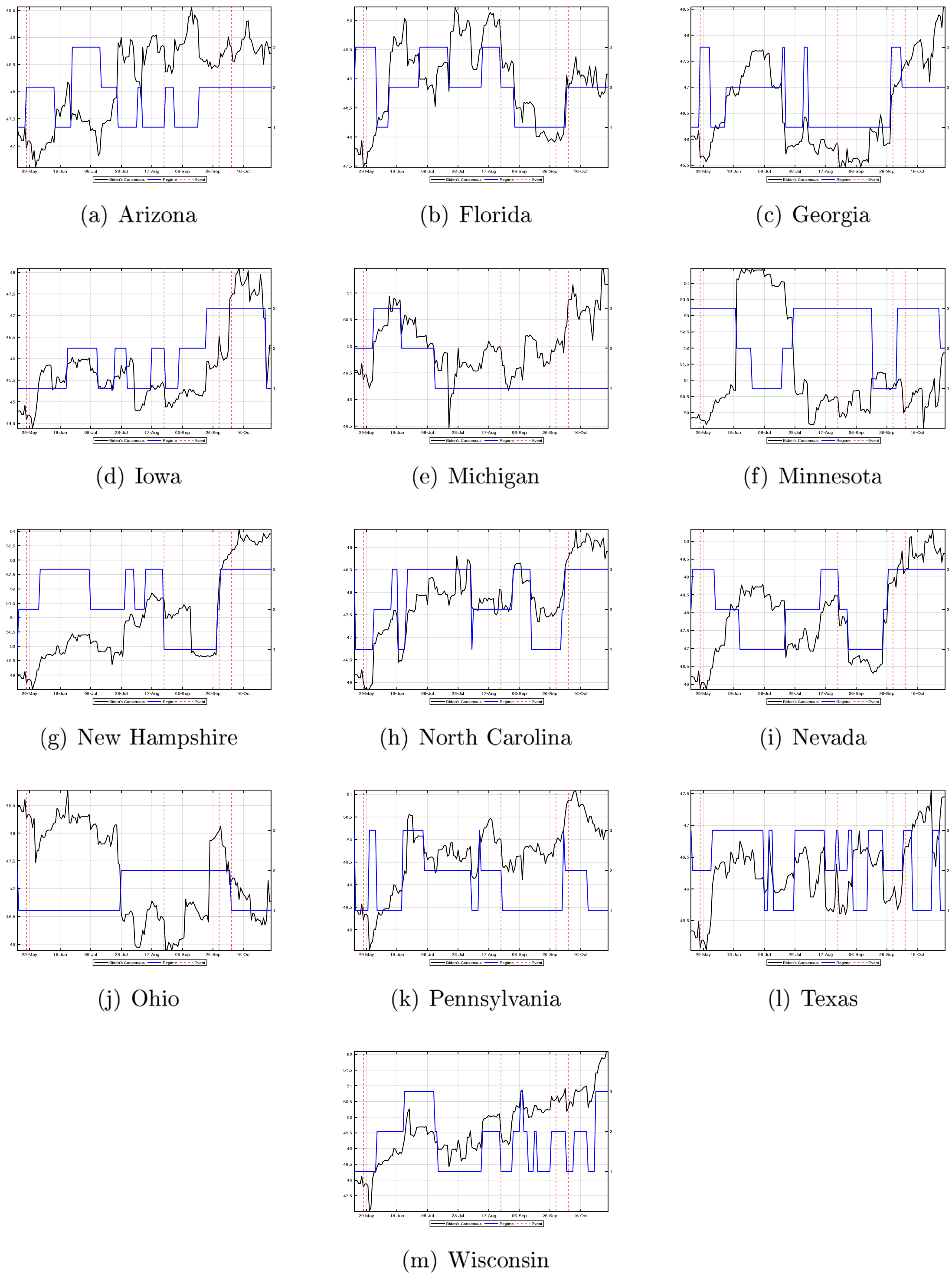

Fig. 4. Presidential polling data in favor of Biden (black line on the left axis), prevailing regime (blue line on the right axis), and exogenous events (red vertical dashed-lines). Sample period May 20, 2020–November 3, 2020.

areas, and a strong cultural conservatism among key voter groups. Despite being geographically distant, these states often exhibit similar reactions to nationwide debates on issues like immigration, public safety, and economic uncertainty, which are particularly salient in Florida's political landscape. Interestingly, Wisconsin is influenced by North Carolina and Pennsylvania, given the relevance

Table 6
Influential states for the construction of the vector $\boldsymbol{w}_{s,j}$, identified by applying the recursive algorithm (weights in parentheses).

Swing state	Influential states (weights)
Arizona	–
Florida	Arizona (0.259), Missouri (0.500), Pennsylvania (0.241)
Georgia	Nebraska (0.597), Pennsylvania (0.403)
Iowa	Montana (0.975), New Mexico (0.025)
Michigan	Kentucky (0.714), Montana (0.066), Tennessee (0.220)
Minnesota	Arizona (0.079), Indiana (0.522), Nebraska (0.398)
Nevada	Colorado (0.448), Massachusetts (0.552)
New Hampshire	Kentucky (0.771), Massachusetts (0.218), Pennsylvania (0.011)
North Carolina	Arizona (0.061), Montana (0.905), Washington (0.034)
Ohio	North Dakota (0.998), Washington (0.002)
Pennsylvania	Massachusetts (0.023), West Virginia (0.977)
Texas	North Dakota (0.294), Utah (0.003), West Virginia (0.703)
Wisconsin	Maine (0.241), North Carolina (0.545), Pennsylvania (0.214)

Table 7
Second stage: ARX estimated coefficients and robust standard error (White, 1980) in parentheses (panel a). Panel (b) reports the p-values for the Ljung–Box statistics. P-values for the ARCH-LM test for residual heteroskedasticity (Engle, 1982) is reported in panel (c). Sample period: 20 May, 2020–November 3, 2020.

	Estimation output												
(a)	Arizona	Florida	Georgia	Iowa	Michigan	Minnesota	Nevada	New Hampshire	North Carolina	Ohio	Pennsylvania	Texas	Wisconsin
ω	−0.0139	−0.0598	−0.0187	−0.0203	−0.0018	−0.0259	−0.0554	−0.1111	−0.0988	0.0403	−0.0206	−0.0472	−0.0053
	(0.0003)	(0.0006)	(0.0008)	(0.0003)	(0.0003)	(0.0003)	(0.0004)	(0.0008)	(0.0005)	(0.0006)	(0.0003)	(0.0004)	(0.0003)
φ	0.7055	0.4962	0.2791	0.7677	0.7202	0.6070	0.6408	0.1725	0.5613	0.3951	0.6734	0.3182	0.5970
	(0.0004)	(0.0011)	(0.0005)	(0.0004)	(0.0005)	(0.0005)	(0.0005)	(0.0010)	(0.0006)	(0.0008)	(0.0005)	(0.0007)	(0.0005)
θ_s		−0.1619	1.3592	−0.0076	0.0026	0.3872	−0.0396	0.2367	0.1555	0.0621	0.0571	0.1451	0.2672
		(0.0010)	(0.0049)	(0.0004)	(0.0005)	(0.0007)	(0.0005)	(0.0006)	(0.0005)	(0.0004)	(0.0003)	(0.0004)	(0.0007)
θ_c	0.4812	0.4709	−1.1942	0.6150	0.6232	0.3830	0.7722	0.3890	0.7742	0.5974	0.4335	0.5933	0.6182
	(0.0016)	(0.0014)	(0.0023)	(0.0011)	(0.0016)	(0.0013)	(0.0011)	(0.0009)	(0.0016)	(0.0017)	(0.0015)	(0.0018)	(0.0008)
(b)	Ljung–Box statistics: p-value												
LB 1	0.7670	0.4271	0.7487	0.8253	0.3895	0.4402	0.8082	0.6767	0.9248	0.8025	0.6877	0.6479	0.2804
LB 2	0.4523	0.4912	0.1470	0.6071	0.6905	0.2327	0.4127	0.4406	0.9953	0.8330	0.9172	0.5116	0.3229
LB 3	0.4980	0.5026	0.1368	0.7962	0.4249	0.3951	0.5812	0.4819	0.9027	0.8521	0.9190	0.7166	0.4172
LB 4	0.2740	0.4408	0.1724	0.9051	0.5904	0.5332	0.6543	0.6115	0.9007	0.9349	0.9637	0.7410	0.5840
LB 5	0.1840	0.3273	0.2650	0.8309	0.6781	0.1406	0.7833	0.7401	0.9576	0.6914	0.9370	0.1552	0.7232
(c)	ARCH test: p-value												
	0.8448	0.0842	0.9994	0.9640	0.2795	0.9981	0.5805	0.0088	0.8151	0.0139	0.0002	0.0050	0.0977

of working-class voters in these regions and the historical alignment of these swing states of the Rust Belt. Similarly, the influence of Colorado on Nevada probably reflects shared demographic and cultural trends, including recent shifts towards the Democratic Party. The case of Michigan being influenced by Kentucky and Tennessee is also plausible, as these states are geographically close and have all experienced increasing political polarization in recent electoral cycles. However, some relationships appear less intuitive: the influence of Nebraska on Georgia may seem surprising, considering the limited political and demographic similarity between the two states, but this relationship could reflect a broader phenomenon related to changes in suburban votes and ongoing electoral dynamics. Likewise, the impact of North Dakota on Ohio and Texas seems unusual, given North Dakota's smaller electoral weight and relatively isolated political dynamics.

After identifying the vectors $\boldsymbol{w}_c$ and $\boldsymbol{w}_s$, in the second stage, the estimation results of the ARX indicate a strong degree of heterogeneity across different states, particularly in the magnitude and direction of spatial spillover and contagion effects. More specifically, Table 7 presents the estimated parameters along with the corresponding robust standard errors (in parentheses). The coefficient $\hat{\varphi}$ is consistently positive across all specifications, with values ranging from 0.17 to 0.77, indicating a medium/strong autoregressive component in the process and suggesting that past observations significantly influence current values. The coefficient $\hat{\theta}_s$ captures spatial spillover effects originating from other states: when estimated, it shows substantial variation, with values ranging from −0.162 to 1.359. In particular, Florida has a negative spillover effect, with an estimate of −0.162, suggesting that Biden's support in other swing states had a lower influence on Florida compared to other swing states. Keeping an eye on the outcome of the election and the sources of political spillover (cf. Table 6), it is not surprising that $\hat{\theta}_s$ is positive for some states such as Minnesota, North Carolina, Ohio, and Texas. Moreover, the negative coefficient for Florida, Iowa, Nevada is partially justified by the influence of some politically divergent states such as North Carolina and Montana for Florida, Massachusetts for Nevada, Montana and New Mexico for Iowa.

Finally, the presence of missing estimates for Arizona implies that no influential states were identified according to the selection algorithm described at the end of Section 3.2. The coefficient $\hat{\theta}_c$ captures the effect of contagion, measuring how the consensus of Biden in state j changes due to the influence of neighboring states. Estimates range from −1.194 to 0.772, indicating a significant variation in the strength and direction of the contagion effect between states. For example, Georgia has a negative value for $\hat{\theta}_c$, implying that Biden's support in Georgia increased when a decline was observed in its neighboring states. This result aligns with the election outcome, as Biden won in Georgia while losing in all its bordering states: Florida, Alabama, Tennessee, North Carolina, and South Carolina. The explanation for this result lies in the fact that Georgia is subject to significant demographic changes, especially in the Atlanta metropolitan area, with a rapid expansion of its suburbs. The 2020 elections were characterized by a strong effort to increase minority voter registration, thanks to the action of Stacey Abrams, a local African-American politician, and of grassroots groups, such as the New Georgia Project. This campaign was so successful that also led to the election of two new Democratic senators, whose victories ensured control of Congress for the Democrats.

Panel (b) reports the *p*-values for the Ljung–Box statistics. For all lags considered, we do not reject the null hypothesis of no autocorrelation at the 1% significance level, suggesting that the estimated model effectively captures the dynamics of the polling time series. Finally, panel (c) presents the *p*-values for the ARCH-LM test for residual heteroskedasticity (Engle, 1982). Identifying different variances in different regimes helps capture heteroskedasticity; in fact, the null hypothesis is not rejected at the significance level 1% in all cases except New Hampshire, Pennsylvania, and Texas. The presence of heteroskedasticity in the residuals may be interpreted as a sign of greater uncertainty or volatility in voter sentiment over time, particularly in more competitive or politically unstable states. However, if we add a simple GARCH(1,1) (Bollerslev, 1986) equation to represent the time-varying conditional variance of these series, we obtain standardized residuals unaffected by heteroskedasticity.

In conclusion, these findings support the effectiveness of the proposed two-step estimation approach in capturing both temporal and spatial dependencies in the data. The results confirm that electoral polls reflect complex dynamics characterized by regime changes and spatial interactions: the integration of MS and ARX models captures both the temporal dimension — where key political events determine distinct phases in the evolution of preferences — and the spatial dimension, emphasizing how geographic proximity and connectivity among states can amplify or mitigate these variations.

5. Final remarks

Statistical analysis can shed light in the understanding of the formation of electoral results, linking their evolution to temporal dynamics and spatial interactions. In this work, we propose a novel approach, based on MS and ARX models, with spatial effects, analyzing the polls in favor of Biden in the so-called swing states during the 2020 electoral campaign. The basic intuition is that the dynamics of polls in each state contain segmented trends, corresponding to periods of decline, stability, and growth, with cases of abrupt changes (level shifts), which are lost when transforming the series to obtain stationary models for classical time series analysis. To this end, we proposed a 2-stage model, with a first stage dedicated to capturing segmented trends, having the possibility of relating turning points to exogenous electoral events; a second stage in which we detrend the series based on the estimated trends of the first stage, having the possibility of analyzing the spatial–temporal evolution of individual state polls.

The results are encouraging. The interpretation of the changes in regime seems consistent with some particular events that characterized the electoral campaign. We considered several potential influential events, identifying four that seem more related to the inference on regime: Biden reaching the delegate threshold, the beginning of the Republican convention, the presidential debate, and the vice-presidential debate. Interestingly, this new way of detrending the series provides stationary time series, which have a very simple autoregressive structure: an AR(1) model with spatial effects can capture the residual structure of the series (as shown by the Ljung–Box test on the final residuals), leaving only a residual heteroskedasticity in four time series (New Hampshire, Pennsylvania and Texas), captured by adding a GARCH equation. We propose to include two types of spatial effects: the spillover effect, due to the transmission of changes from a subset of influential states with a lag (a sort of space–time effect); the contagion effect, due to the purely spatial influence of neighbors. The latter is significantly present in all the analyzed series. For the former, we propose an algorithm to select the influential series; the algorithm find no influential states for Arizona, but for the remaining twelve cases, the spillover effect is significant. A clear example of spatial interpretation of the results is represented by Georgia; this is consistent with the final vote illustrated in Figs. 1 and 3: Georgia voted for the Democratic candidate surrounded by Republican-leaning states.

The main message from our results is that knowledge of the presence of local trends (in favor of one of the two candidates) can justify to engage in increasing efforts in the electoral campaign of specific states to consolidate or modify such a trend. More importantly, the presence of spatial clustering gives an important insight into the fact that electoral actions in neighboring states has an effect on a state's outcome. In particular, the study of spillover effects — i.e. irrespective of geographic proximity — could lead to the design of electoral actions in states identified as influential; knowledge that the effects extend to other states, especially swing states, which are more sensitive to changes in the vote is one of the novel outcomes of our approach.

Unfortunately, our dataset is not complete; we had to exclude 11 states from the analysis due to a lack of data for this type of analysis. The same data source contains data for the 2024 election polls, but the problem of missing data is even more dramatic.

An interesting extension of the approach would be a multivariate analysis with a single model for all states. The feasibility problem arises due to the dramatic increase in unknown coefficients, which requires a reparameterization to reduce them (e.g., using the clustering of parameters in space–time series proposed by D'Urso et al., 2022). The further difficulty is due to the different regime changes for each state, which implies the impossibility of adopting the same Markov chain for all series. A possible solution could be an extension of the multi-chain MS model (Otranto, 2005; Gallo and Otranto, 2008). Alternatively, an ad hoc solution could be to consider univariate MS models in the first stage and a multivariate ARX model in the second stage.

Funding statement

Financial support is acknowledged by Otranto: Italian PRIN 2022 grant (20223725WE) "Methodological and computational issues in large-scale time series models for economics and finance". The views and opinions expressed are solely those of the authors and do not necessarily reflect those of the EU, nor can the EU be held responsible for them.

Declaration of competing interest

The authors declare that they have no known competing financial interests or personal relationships that could have appeared to influence the work reported in this paper.

Acknowledgments

The Authors are grateful to the Conference participants at ICES 2025 in Naples (Feb. 13-14, 2025) and at the “Disinformazione e Scienze dei Dati Elettorali” held in Rome (Mar. 20, 2025) for valuable comments; they thank Luca Scaffidi Domianello for useful discussions and insights.

References

Agnew, J.A., 1987. Place and Politics: The Geographical Mediation of State and Society. Allen & Unwin, Boston.
Anselin, L., 2013. Spatial Econometrics: Methods and Models, vol. 4, Springer Science & Business Media.
Berlemann, M., Enkelmann, S., 2014. The economic determinants of US presidential approval: A survey. Eur. J. Political Econ. 36, 41–54.
Bollerslev, T., 1986. Generalized autoregressive conditional heteroskedasticity. J. Econometrics 31, 307–327.
Dickey, D.A., Fuller, W.A., 1979. Distribution of the estimators for autoregressive time series with a unit root. J. Amer. Statist. Assoc. 74 (366), 427–431.
Dong, H., Yu, W., Cao, Z., Ma, Q., 2020. A survey on ensemble learning. Front. Comput. Sci. 14, 241–258.
D’Urso, P., 2015. Fuzzy clustering. In: Hennig, C., Meila, M., Murtagh, F., Rocci, R. (Eds.), Handbook of Cluster Analysis. Chapman and Hall, pp. 545–566.
D’Urso, P., Mucciardi, M., Otranto, E., Vitale, V., 2022. Community mobility in the European regions during covid-19 pandemic: a partitioning around medoids with noise cluster based on space–time autoregressive models. Spat. Stat. 49, 100531.
Elhorst, J., Lacombe, D., Piras, G., 2012. On model specification and parameter space definitions in higher order spatial econometric models. Reg. Sci. Urban Econ. 42, 211–220.
Engle, R.F., 1982. Autoregressive conditional heteroscedasticity with estimates of the variance of United Kingdom inflation. Econometrica 50, 987–1007.
Foley, P., Demšar, U., 2013. Using geovisual analytics to compare the performance of geographically weighted discriminant analysis versus its global counterpart, linear discriminant analysis. Int. J. Geogr. Inf. Sci. (4), 633–661.
Gallo, G.M., Otranto, E., 2008. Volatility spillovers, interdependence and comovements: A Markov switching approach. Comput. Statist. Data Anal. 52 (6), 3011–3026.
Geary, R., 1954. The contiguity ratio and statistical mapping. Inc. Stat. 5, 115–145.
Hamilton, J., 1990. Analysis of time series subject to changes in regime. J. Econometrics 45, 39–70.
Hamilton, J.D., 1994. Time Series Analysis. Princeton University Press.
Hamilton, J., Susmel, R., 1994. Autoregressive conditional heteroskedasticity and changes in regime. J. Econometrics 50, 307–333.
Hansen, B., 1992. The likelihood ratio test under nonstandard conditions: Testing the Markov switching model of GNP. J. Appl. Econometrics 7 (s), 61–82.
Hubert, L., Arabie, P., 1985. Comparing partitions. J. Classification 2, 193–218.
Kim, C., 1994. Dynamic linear models with Markov switching. J. Econometrics 60, 1–22.
Moran, P., 1948. The interpretation of statistical maps. J. R. Stat. Soc. Ser. B 10, 243–251.
Otranto, E., 2005. The multi-chain Markov switching model. J. Forecast. 24, 523–537.
Otranto, E., Scaffidi Domianello, L., 2025. On using fuzzy clustering for detecting the number of states in Markov switching models. Ann. Oper. Res. 349 (3), 1855–1890.
Pattie, C., Johnston, R., 2000. ‘People who talk together vote together’: An exploration of contextual effects in Great Britain. Ann. Assoc. Am. Geogr. 90 (1), 41–66.
Psadarakis, Z., Spagnolo, N., 2003. On the determination of the number of regimes in Markov-Switching autoregressive models. J. Time Series Anal. 24, 237–252.
Psadarakis, Z., Spagnolo, N., 2006. Joint determination of the state dimension and autoregressive order for models with Markov regime switching. J. Time Series Anal. 27, 753–766.
Rand, W.M., 1971. Objective criteria for the evaluation of clustering methods. J. Amer. Statist. Assoc. 66 (336), 846–850.
White, H., 1980. A heteroskedasticity-consistent covariance matrix estimator and a direct test for heteroskedasticity. Econometrica 48 (4), 817–838.
Wing, I.S., Walker, J.L., 2010. The geographic dimensions of electoral polarization in the 2004 US presidential vote. Prog. Spat. Anal.: Methods Appl. 253–285.